

THE EFFECT OF Co AND Ni IN HYDRODESULPHURIZATION OF BENZO[b]THIOPHENE ON Mo AND W CATALYSTS

Rudolf PETER and Miroslav ZDRAŽIL

*Institute of Chemical Process Fundamentals,
Czechoslovak Academy of Sciences, 165 02 Prague 6 — Suchbát*

Received July 12th, 1985

Hydrodesulphurization of benzo[b]thiophene (BT) on sulphided Mo, W, Co-Mo, Co-W, Ni-Mo, and Ni-W catalysts has been studied at total pressure 2.1 MPa and temperature 543 K. The catalysts were laboratory preparations with alumina or active carbon as a support and also commercial samples. The formation of intermediate 2,3-dihydrobenzo[b]thiophene (DHBT) was observed with all catalysts. On non-promoted catalysts, large quantities of it were formed; partial equilibrium BT-DHBT-H₂ was attained already at low desulphurization conversions. On promoted catalysts (Co-W, Co-Mo, Ni-W, Ni-Mo) the amount of DHBT formed was small; the partial equilibrium BT-DHBT-H₂ was not attained even at high desulphurization conversions. The data were correlated by kinetic equations derived from consecutive reaction scheme assuming steady state conditions for adsorbed species. The separation of individual reaction steps was not possible and only formal kinetic constants were obtained. It was concluded that the effect of Co or Ni in the reaction sequence is localized in the steps between partially hydrogenated BT on the surface and gaseous hydrogen sulphide and hydrocarbons.

The effect of Co or Ni promoter in hydrodesulphurization (HDS) has been extensively studied mainly with emphasis on the inorganic chemistry of the catalysts (for review see refs¹⁻⁵). Such approach gives only little information on the role of the promoter in the reaction sequence and the understanding of the mechanism, by which the promoter increases the overall rate, is still very limited. The comparison of the distribution of reaction intermediates on non-promoted and promoted catalysts might contribute to the better insight into this mechanism.

In our previous communications^{6,7}, we have observed a great difference in the formation of 2,3-dihydrobenzo[b]thiophene (DHBT) in HDS of benzo[b]thiophene (BT) on non-promoted and Co or Ni promoted Mo catalysts. The formation of DHBT was extensive on Mo/Al₂O₃ and small on Co-Mo/Al₂O₃ and Ni-Mo/Al₂O₃ catalysts. This indicates that promoter directly influences only a part of the reaction sequence, namely the steps between partially hydrogenated BT on the surface and hydrogen sulphide and hydrocarbon in gas phase. The first purpose of the present work is to report on our progress in further generalization of this observation. The behaviour of Mo based catalysts supported on alumina was compared with Mo based catalysts supported on carbon and with W based catalysts supported on alumina.

Most authors assume that hydrogen sulphide is formed during HDS of BT by two parallel ways, the first involving DHBT as an intermediate and the second being "direct hydrogenolysis" of BT (*e.g.*⁸⁻¹¹). We advocate the consecutive hydrogenation-elimination mechanism which does not involve "direct hydrogenolysis" step¹². We have found recently, that such mechanism conforms to the integral kinetic data obtained at atmospheric pressure⁷. The second purpose of the present paper is to show that this holds also for data measured at 2.1 MPa.

EXPERIMENTAL

The composition of the studied catalysts is shown in Table I. The carriers used for preparation of laboratory samples were γ -alumina CHEROX 33-00 (Chemical Works, Litvínov, Czechoslovakia) and active carbon CAL 12-14 (Pittsburgh Activated Carbon, U.S.A.). They were crushed and sieved to the particle size 0.16-0.25 mm before impregnation. The slurry of a solution of an appropriate salt (ammonium molybdate, ammonium tungstate) with the carrier was dried in a rotary evaporator under reduced pressure at 373 K. Promoter salts (cobalt nitrate or nickel nitrate) were impregnated in the same way using dried non-promoted catalyst instead of

TABLE I
Catalysts and their composition^a

Catalyst	Composition %			
	MoO ₃	WO ₃	NiO	CoO
Co/Al ₂ O ₃	—	—	—	3.0
Ni/Al ₂ O ₃	—	—	3.0	—
Mo/Al ₂ O ₃	8.6	—	—	—
Co-Mo/Al ₂ O ₃	8.6	—	—	2.5
Ni-Mo/Al ₂ O ₃ (I)	8.6	—	0.1	—
Ni-Mo/Al ₂ O ₃ (II)	8.6	—	0.8	—
Ni-Mo/Al ₂ O ₃ (III)	8.6	—	2.5	—
W/Al ₂ O ₃	—	15	—	—
Ni-W/Al ₂ O ₃	—	15	2.5	—
Co-W/Al ₂ O ₃	—	15	—	2.5
Co/C	—	—	—	6.0
Mo/C	16	—	—	—
Co-Mo/C	15	—	—	6.0
Cherox 3601 ^b	13	—	—	3.5
Cyanamid Trilobe HDS-20 ^c	15	—	—	5.0
Harshaw HT-400E ^d	15	—	—	3.0

^a For commercial samples approximate values according producers's literature. ^b Chemical Works ČSSP, Litvínov, Czechoslovakia. ^c American Cyanamid Co., Texas, U.S.A.. ^d The Harshaw Chemical Co., Cleveland, U.S.A.

pure carrier. Alumina supported catalysts were calcined for 3 h at 823 K in a flow of air and carbon supported samples were not calcined. Commercial catalysts were crushed and sieved to the particle size 0.16–0.25 mm.

All catalysts were presulphided by the mixture $\text{H}_2\text{S} + \text{H}_2$ (1 : 10) at 720 K by the procedure described elsewhere¹³ and were stored in air. Several runs with samples in oxidic form were also made for comparison.

The experiments were conducted in a down-flow, stainless steel tubular reactor with i.d. either 4 or 8 mm, depending on the catalyst charge W . Benzo[b]thiophene (Fluka, redistilled) was fed by a piston pump as a 16.6 mol % solution in *n*-decane (Reachim, rectified). The total pressure was 2.1 MPa and the molar ratio hydrogen : decane : BT was 46.5 : 5 : 1. It was calculated that no liquid phase should be present in the reactor under the reaction conditions. The lowest feed rate F of BT was 0.01 mol h^{-1} . It was checked that the results obtained with this and higher F were not influenced by external mass transport limitations: activity and selectivity (the extent of DHBT formation) at a given space time W/F was independent of the catalyst charge. It was further assumed that the catalyst particles were small enough to exclude internal mass transport effects on activity and selectivity.

The condenser at the reactor outlet was cooled to 263 K and liquid products were analyzed by GLC (1.7 m column packed with 20% Apiezon L on Rysorb BLK operating at 473 K). The good efficiency of the condenser was checked in experiments without a catalyst in the reactor. The results were expressed in terms of molar fractions of BT, DHBT and H_2S in the reaction mixture *vs* space time. Molar fractions were defined: $a(\text{BT}) = n(\text{BT})/n^\circ(\text{BT})$, $a(\text{DHBT}) = n(\text{DHBT})/n^\circ(\text{BT})$, and $a(\text{HS}) = n(\text{HS})/n^\circ(\text{BT})$, where $a(i)$ is molar fraction of the component i , n and n° are moles in the products and feed, respectively, and HS is H_2S . The values of $a(\text{BT})$ and $a(\text{DHBT})$ were determined by GLC analysis and $a(\text{HS})$ was calculated from the balance $a(\text{BT}) + a(\text{DHBT}) + a(\text{HS}) = 1$.

The catalyst charge (0.15–15 g) was placed in the reactor and was heated in hydrogen at 2.1 MPa during 50 min to 543 K and was kept at this temperature for 1 h. The feeding of the liquid was started and a steady state in the composition of the liquid products was attained after approx. 30 min. The composition data $a(\text{BT})$ and $a(\text{DHBT})$ for each value of W/F were obtained with a fresh catalyst charge.

RESULTS

General Features of the Data and their Kinetic Correlation

The results of experiments were integral dependences of $a(\text{BT})$ and $a(\text{DHBT})$ on space time W/F ($\text{kg}(\text{cat}) \text{ h mol}(\text{BT})^{-1}$) at constant temperature, total pressure and feed composition. They were measured on most catalysts in the broad range of $a(\text{BT})$ from 1 to 0. The main features of data and their mathematical treatment will be shown on results obtained with $\text{Mo}/\text{Al}_2\text{O}_3$ and $\text{Ni-Mo}/\text{Al}_2\text{O}_3$ (III) catalysts. These results are a prototype of behaviour for all other pairs of non-promoted – promoted catalysts.

The integral dependences of $a(i)$ *vs* space time for these two catalysts are shown in Fig. 1a. It is seen that the promoter increases the rate of H_2S formation more than the rate of BT disappearance and that it substantially suppresses DHBT desorption.

The effect of promoter on DHBT formation is further conveniently described in Fig. 1b where the values of $a(i)$ are plotted in the reaction triangle not containing space time. The concept of reaction triangle and related terminology used here was taken from the classical paper by Wei and Prater¹⁴. The total equilibrium in the system BT–DHBT–H₂–(EB + H₂S) at our conditions is given in Fig. 1b by the vertex (H₂S + EB), where EB is ethylbenzene. The partial equilibrium BT–DHBT–H₂ is expressed in Fig. 1b by line **e**. The determination of it will be described below. The composition of the reaction mixture moves from pure BT to the total equilibrium point along the curves referred to as reaction paths. The reaction paths cannot intersect the partial equilibrium line but they can asymptotically approach it.

It is seen in Fig. 1b that the reaction path on Mo/Al₂O₃ catalyst approaches the partial equilibrium line already at low desulphurization conversion ($a(\text{HS}) \cdot 100$) of about 30%. From this value up, further desulphurization proceeds with essentially equilibrium ratio $a(\text{DHBT})/a(\text{BT})$. On the other hand, the reaction path on Ni–Mo/Al₂O₃ (III) catalyst is far from partial equilibrium line even at high desulphurization conversions. The behaviour of all other pairs of non-promoted – promoted catalysts studied in this work also followed this pattern.

The scheme of the reaction used here for the interpretation of the results is shown in Fig. 2. It is the simplest representation of consecutive “hydrogenation-elimination” mechanism of HDS of BT which does not involve “direct hydrogenolysis”

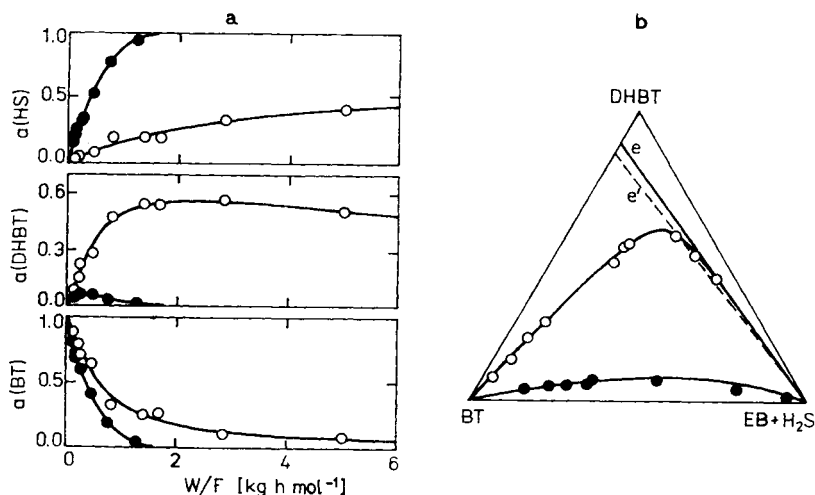


FIG. 1

Typical effect of promoter in HDS of BT at temperature 543 K and pressure 2.1 MPa. **a** Integral curves, **b** reaction paths; ○ Mo/Al₂O₃, ● Ni–Mo/Al₂O₃(III), **e** partial equilibrium line, **e'** partial equilibrium line from experiments at atmospheric pressure⁷

step connecting adsorbed BT and H₂S. Alternative representations of it which are for gas phase kinetics indistinguishable from the scheme in Fig. 2, were mentioned previously⁷. This mechanism is supported by chemical considerations. Available kinetic data, including the data in the present paper, can neither verify nor disprove it. This impossibility of the determination of surface reaction network from gas phase kinetics follows from the well known phenomena referred to as "disguised kinetics" and analyzed by several authors¹⁴⁻¹⁷. The non-kinetic evidence for consecutive hydrogenation-elimination mechanism was summarized elsewhere¹² and the validity of the scheme in Fig. 2 was taken as a postulate in the present work.

In the derivation of kinetic equations we have started from Eqs (1)–(5). These expressions were obtained for the scheme such

$$\frac{db_1}{d(W/F)} = \frac{\lambda_1 b_1}{1 + v_1 b_1 + v_2 b_2} \quad (1)$$

$$\frac{db_2}{d(W/F)} = \frac{\lambda_2 b_2}{1 + v_1 b_1 + v_2 b_2} \quad (2)$$

$$b_1/b_1^0 = (b_2/b_2^0)^{\lambda_1/\lambda_2} \quad (3)$$

$$b_1 = a(\text{BT}) + u_1 a(\text{DHBT}) \quad (4)$$

$$b_2 = a(\text{BT}) + u_2 a(\text{DHBT}) \quad (5)$$

as in Fig. 2 by Wei and Prater under assumption of the steady state condition for surface species¹⁴. Constants λ_1 , λ_2 , v_1 , v_2 , u_1 , and u_2 are complex constants composed from k_{ij} constants in Fig. 2, b_i are auxiliary variables (a hypothetical species), and b_i^0 are their initial values. Further details are available in the original paper¹⁴ and also in our previous work⁷.

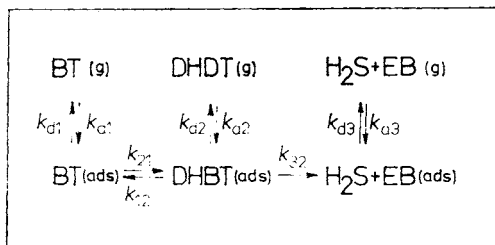


FIG. 2

Scheme of hydrodesulphurization of benzo[*b*]thiophene; (g) gas phase, (ads) adsorbed, k_{ij} rate constants

The function $F(a(\text{BT}), a(\text{DHBT})) = 0$ describing the reaction paths in the reaction triangle was obtained by substitution of Eqs (4) and (5) into Eq. (3). The reaction paths are thus determined by three constants u_1 , u_2 , and λ_1/λ_2 .

The functions $G(a(\text{BT}), W/F) = 0$ and $H(a(\text{DHBT}), W/F) = 0$ describing the space time dependences of molar fractions were obtained by integration of Eq. (1) using Eq. (3) to eliminate b_2 . The integration gives

$$\lambda_1(W/F) = \ln |b_1/b_1^0| + v_1(b_1 - b_1^0) + v_2 b_2^0 (\lambda_1/\lambda_2) ((b_1/b_1^0)^{(\lambda_1/\lambda_2)} - 1) \quad (6)$$

and this expression together with Eqs (3), (4), and (5) determines the required functions H and G . The space time dependence of composition is thus determined by six constants v_1 , v_2 , u_1 , u_2 , λ_1 , and λ_1/λ_2 .

The constants k_{ij} in Fig. 2 are of course always positive and this gives the following limitations to the values of composed constants: u_1 and λ_1 must be negative, u_2 and λ_1/λ_2 must be positive and the signs of v_1 and v_2 are not restricted. The values of constants u_1 and u_2 must further fulfil the relation

$$\frac{a^*(\text{DHBT})}{a^*(\text{BT})} = \frac{k_{a1}k_{d2}k_{21}}{k_{d1}k_{a2}k_{12}} = -\frac{1}{u_1u_2}, \quad (7)$$

where $a^*(i)$ are partial equilibrium values. The value of the partial equilibrium ratio $a^*(\text{DHBT})/a^*(\text{BT})$ must be the same for all catalysts. The way of the determination of the value of it used in the fitting procedure is explained below.

The data for each catalyst were fitted in two steps. In the first one, the constants u_1 , u_2 , and λ_1/λ_2 were obtained by fitting the reaction paths by Eqs (3)–(5). In the second step the constants λ_1 , v_1 , and v_2 were obtained by fitting the space time dependences of mole fractions by Eqs (3)–(6), using the constants u_1 , u_2 , and λ_1/λ_2 calculated in the first step. The constants obtained for $\text{Mo}/\text{Al}_2\text{O}_3$ and $\text{Ni-Mo}/\text{Al}_2\text{O}_3$ (III) catalysts are presented in Table II and the curves calculated using them are shown in Fig. 1.

Numerical Results

The results for all remaining catalysts are shown in Figs 3–6. The number of experimental points and the quality of fit was in all cases comparable to that shown in Fig. 1 for $\text{Mo}/\text{Al}_2\text{O}_3$ and $\text{Ni-Mo}/\text{Al}_2\text{O}_3$ (III) catalysts. In this situation, the experimental points are not shown in Figs. 3–6 in order to keep the results easily to survey. The values of constants u_1 , u_2 , v_1 , v_2 , λ_1 , and λ_1/λ_2 obtained for all catalysts and used to calculate the curves in Figs 3–6 fulfilled all the limitations mentioned above (restrictions of sign and validity of Eq. (7)). The values are not presented here because

the complex physical meaning of the constants makes the discussion of values obtained impossible (see also Discussion).

The partial equilibrium $a^*(\text{DHBT})/a^*(\text{BT})$ binding together the values of u_1 and u_2 by Eq. (7) must be independent of the catalyst. The value of it which is needed in fitting procedure was determined from data on non-promoted catalysts $\text{W}/\text{Al}_2\text{O}_3$, $\text{Mo}/\text{Al}_2\text{O}_3$, and Mo/C . On these catalysts, the ratio $a(\text{DHBT})/a(\text{BT})$ converged at

TABLE II

Kinetic constants in Eqs (3)–(6) describing HDS of BT at pressure 2.1 MPa and temperature 543 K

Catalyst	Constant ^a					
	u_1	u_2	λ_1/λ_2	λ_1	v_1	v_2
$\text{Mo}/\text{Al}_2\text{O}_3$	-0.11	1.06	8.27	-1.85	0.186	-1.03
$\text{Ni-Mo}/\text{Al}_2\text{O}_3(\text{III})$	-5.03	0.023	2.49	-144	-6.15	6.54

^a Dimension of λ_1 is $(\text{mol}(\text{BT}) (\text{kg}(\text{cat}))^{-1} \text{h}^{-1})$, other constants are dimensionless.

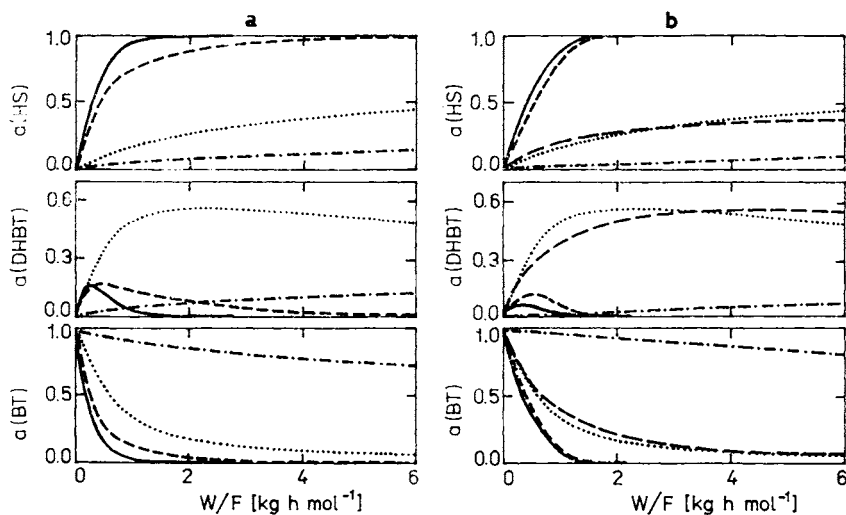


FIG. 3

Effect of cobalt and nickel in HDS of BT on Mo based catalysts supported on alumina. *a* $\text{Mo}/\text{Al}_2\text{O}_3$, - - - - $\text{Co}/\text{Al}_2\text{O}_3$, - - - - Cherox 3601, - - - - $\text{Co-Mo}/\text{Al}_2\text{O}_3$; *b* $\text{Mo}/\text{Al}_2\text{O}_3$, - - - - $\text{Ni}/\text{Al}_2\text{O}_3$, - - - - $\text{Ni-Mo}/\text{Al}_2\text{O}_3(\text{I})$, - - - - $\text{Ni-Mo}/\text{Al}_2\text{O}_3(\text{II})$, - - - - $\text{Ni-Mo}/\text{Al}_2\text{O}_3(\text{III})$

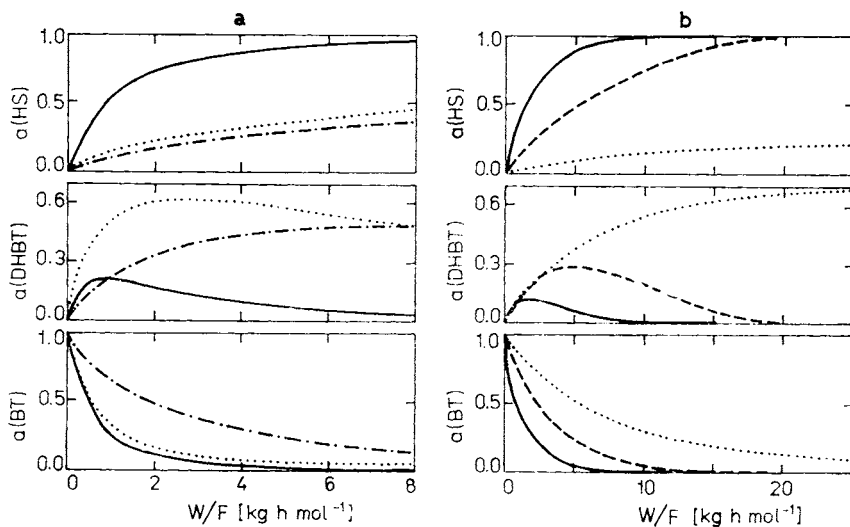


FIG. 4

Effect of promoter in HDS of BT on carbon supported Mo catalysts and on alumina supported W catalysts. **a** Mo/C, - - - - Co/C, — Co-Mo/C; **b** W/Al₂O₃, - - - - Co-W/Al₂O₃, — Ni-W/Al₂O₃

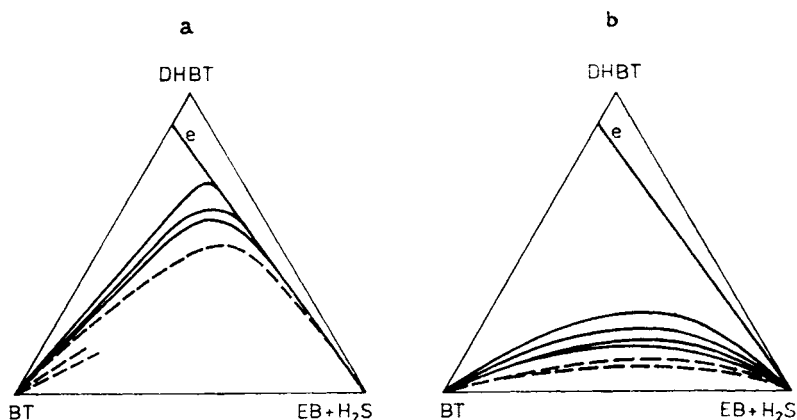


FIG. 5

Reaction paths of HDS of BT at temperature 543 K and pressure 2.1 MPa; **a** non-promoted catalysts and promoters alone, reaction paths from top down: — W/Al₂O₃, Mo/C, Mo/Al₂O₃, - - - - Co/C, Co/Al₂O₃, Ni/Al₂O₃; **b** promoted catalysts, reaction paths from the top down: — Co-W/Al₂O₃, Co-Mo/C, Cherox 3601, Co-Mo/Al₂O₃, - - - - Ni-W/Al₂O₃, Ni-Mo/Al₂O₃(III); **e** partial equilibrium line

high W/F to the constant value 8.6 and this value was taken as $a^*(\text{DHBT})/a^*(\text{BT})$. Fig. 1*b* shows that the partial equilibrium line thus obtained is in a very good agreement with the line calculated from partial equilibrium constant determined previously at atmospheric pressure⁷.

Only two points of integral curve $a(i)$ vs W/F were measured on the commercial catalysts HDS-20 and HT-400E. Their activity was different but the points $a(\text{DHBT}) - a(\text{BT})$ precisely fitted the reaction path for laboratory Co-Mo/Al₂O₃ catalyst.

Several experiments with oxidic forms of catalysts were also made. The catalysts Mo/Al₂O₃, Co-Mo/Al₂O₃, Cherox 3601, and HT-400E were used in these runs. As expected, the activity was always considerably lower as compared to the presulphided samples. The difference in activities of both forms was higher for promoted than for non-promoted samples. This fact was discussed in more detail elsewhere¹⁸. As for DHBT formation, the composition of the reaction mixture required more time on stream to reach a steady state than on presulphided samples. However, after 3 h on stream, the composition of the products fitted well the reaction path for corresponding presulphided sample.

The effect of solvent and of initial partial pressure of BT on the reaction path $a(\text{DHBT}) - a(\text{BT}) - a(\text{HS})$ was tested on catalyst Cherox 3601. The effect of solvent was small, the maximum value of $a(\text{DHBT})$ was 0.19 and 0.17 with aliphatic decane and aromatic mesitylene, respectively. The decrease of the initial partial pressure of BT from 40 kPa to 21 kPa resulted in the more distinct shift of the reaction path, the maximum value of $a(\text{DHBT})$ being 0.19 and 0.12, respectively.

DISCUSSION

The purpose of the present paper was not to evaluate the reaction mechanism by kinetic analysis; we postulated the validity of the hydrogenation-elimination mecha-

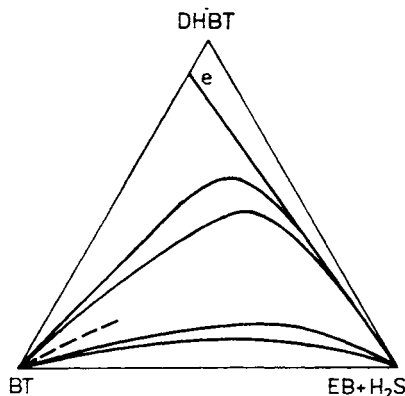


FIG. 6

Effect of the amount of promoter on reaction path of HDS of BT; reaction paths from the top down: ——— Mo/Al₂O₃, Ni-Mo/Al₂O₃(I), Ni-Mo/Al₂O₃(II), Ni-Mo/Al₂O₃(III), - - - - Ni/Al₂O₃; e partial equilibrium line

nism. However, the interpolation of experimental points required the application of some kinetic equation. The data were very well correlated by equations derived from consecutive reaction scheme assuming steady state condition for adsorbed species. This kinetics, not assuming adsorption-desorption equilibrium, has not been applied to HDS previously (for a review of HDS kinetics see *e.g.*¹⁹). Our experience with it was very positive.

The increase of HDS activity upon the addition of Co or Ni to Mo or W catalysts and of alumina and carbon supported catalysts has been compared by other authors (for recent review see⁴). It was not the purpose of this work to study these effects. However, it is worthwhile to comment on the impact of the complexity of the reaction on the evaluation of activity. The rates of BT removal and of H₂S formation are quite different for some catalysts because of the accumulation of sulphur in the form of DHBT. This makes the characterization of the catalyst activity by only one parameter impossible. *E.g.*, the activities of Mo/C and Co-Mo/C catalysts in Fig. 4 are the same as for BT removal but quite different as for H₂S formation. The catalyst Mo/C removes BT easily but it does not desulphurize it; DHBT is formed which reacts only slowly to H₂S. Similar behaviour of other non-promoted catalysts is seen in Figs 3 and 4. As for promoted catalysts, the amount of described DHBT is smaller and the difference between the rate of BT disappearance and H₂S formation is not so high. However, it strongly increases with increasing pressure and the situation for promoted catalysts at pressure 8.5 MPa, ref.¹⁰, is the same as found here for non-promoted catalysts at 2.1 MPa.

The second point concerning activity is the smaller difference between Co/C and Mo/C than between Co/Al₂O₃ and Mo/Al₂O₃ catalysts. This result supports previous conclusions by other authors^{1,3} that low HDS activity of Co/Al₂O₃ (and Ni/Al₂O₃) is caused by metal-alumina interaction and not by properties of the metal sulphide alone.

The effect of promoters on the reaction path was of central interest to this study. The reaction path is an intensive property of catalyst. It is independent of the amount of active sites, provided their quality is the same.

It was observed that the position of the reaction path in the reaction triangle depends strongly on the ratio promoter/principal metal. This is seen in Fig. 6 for the set of Ni-Mo/Al₂O₃ catalysts. The reaction path was proportionally shifted to lower DHBT amounts as the content of Ni increased. It is expected that further addition of Ni, beyond the presumably optimal ratio promoter/principal metal used in commercial catalysts, would not result in further shift of reaction path. Catalysts with optimal amount of promoter produce apparently lowest amount of intermediate DHBT.

The reaction path was found to be insensitive to the details of catalyst preparation. This is shown by results for catalysts of Co-Mo/Al₂O₃ type which all had similar ratio Co/Mo. The catalysts Co-Mo/Al₂O₃, HT-400E and HDS-20 exhibited

identical reaction paths and the catalyst Cherox-3601 only slightly different one, whilst their activities varied substantially. The deviation of Cherox-3601 can be explained by principally different technology of its preparation. It is prepared by co-precipitation and the effective ratio Co/Mo in it might be smaller than for other Co-Mo catalysts prepared presumably by impregnation.

The effect of carrier on reaction path was small but definite. The results obtained on Mo/Al₂O₃-Mo/C, Co/Al₂O₃-Co/C, and Co-Mo/Al₂O₃-Co-Mo/C catalysts showed that larger amounts of DHBT were formed on carbon supported catalysts.

The shift of the reaction path in the reaction triangle reflects the change of ratios of rates in the scheme in Fig. 2. This change cannot be discussed in terms of the k_{ij} values in Fig. 2 because only composed constants were obtained. Two reasons made an evaluation of k_{ij} from u_1 , u_2 , λ_1 , λ_1/λ_2 , v_1 , and v_2 impossible. Firstly, the relations between composed constants and constants k_{ij} are complicated and insufficient to calculate k_{ij} from u_1 , u_2 , λ_1 , λ_1/λ_2 , v_1 , and v_2 . Secondly, some of the composed constants were determined with low accuracy. Other and considerably different sets of constants than those used to calculate the curves in Figs 1, 3-6 fitted the data comparably well. This is a typical experience when kinetic equations with large number of constants are processed. In this situation, we limit ourself only to semiquantitative discussion which further completes and generalizes our previous conclusions based on data measured at atmospheric pressure.

The scheme in Fig. 2 gives no information on the way of the activation of hydrogen and on the nature of catalytic sites. It expresses only key features of the reaction coordinate from the point of view of the organic molecule, the possible intermediates between partially hydrogenated BT on the surface and gaseous H₂S being not shown.

The low desulphurization activity of non-promoted catalysts is caused by a slow step somewhere in the sequence k_{32} , k_{d3} in Fig. 2. The desorption of DHBT(ads) is easier than its further decomposition to H₂S(ads). In this situation the partial equilibrium BT(g)-DHBT(g)-H₂ is attained soon after beginning of the reaction.

The promoter Co or Ni accelerates the rate limiting step of desulphurization in the sequence k_{32} , k_{d3} . The rate of decomposition of DHBT(ads) becomes competitive to the rate of its desorption and the partial equilibrium BT(g)-DHBT(g)-H₂ is not attained.

The rate of BT(g) disappearance is increased by the promoter only indirectly and less than the desulphurization rate. The higher rate of DHBT(ads) decomposition leads to lower concentration of DHBT(ads). This accelerates the rates of the steps BT(g) → BT(ads) and BT(ads) → DHBT(ads) without direct participation of the promoter in these steps.

The position of the equilibrium line and of the reaction path in the reaction triangle for a given catalyst depends strongly on hydrogen pressure and temperature. This was considered as a change of the reaction mechanism⁹. Our interpretation assumes that the mechanism, *i.e.* the chemical nature of all steps in Fig. 2, is in-

dependent of pressure and temperature. What is only changed are relative rates of these steps.

The effect of pressure and temperature was not measured here but can be discussed using previous literature data. These variables determine above all the partial equilibrium line which restricts the course of reaction path. The increase of hydrogen pressure shifts this line in the direction to DHBT vertex and the effect of temperature is opposite. At atmospheric pressure, the ratio $a^*(\text{DHBT})/a^*(\text{BT})$ is about 0.4 at temperature 543 K (ref.⁷) and is expected to be as low as 0.05 at higher temperatures than 623 K. Thermodynamics thus strongly limits the amount of DHBT which can be formed at low pressure and high temperature. On the other hand, at low temperature of about 543 K and high pressure of about 5 MPa the equilibrium line is close to the H₂S–DHBT leg and $a(\text{DHBT})$ is not restricted by thermodynamics.

The effect of hydrogen pressure on the reaction path is made clear by the comparison of this work with data by Daly¹⁰ and our previous paper⁷. The maximum value of $a(\text{DHBT})$ on Co–Mo/Al₂O₃ catalyst at temperature about 540 K was 0.05, 0.20, and 0.80 for hydrogen pressures 0.1, 2.1, and 8.5 MPa, respectively. The increase of $a(\text{DHBT})$ maximum is caused not only by the shift of equilibrium line but also by the fact that the reaction path approaches the equilibrium line more closely. This shows that hydrogen pressure accelerates the steps between BT(g) and DHBT(g) in Fig. 2 much more than the steps between DHBT(ads) and H₂S(g). The effect of hydrogen is thus just opposite to the effect of promoter.

The increase of temperature from 543 to 603 K resulted in a substantial shift of the reaction path to lower $a(\text{DHBT})$ values²⁰. The equilibrium line moves in the same direction (hydrogenation BT → DHBT is exothermic) but no quantitative information on its position at 603 K is available. However, it is assumed that the reaction path approaches equilibrium line more closely at low temperature.

It is also worthwhile to mention that our previous fragmentary data²¹ show the same effect of pressure, temperature, carrier and promoter on the formation of tetrahydrothiophene during HDS of thiophene as discussed above for formation of DHBT.

REFERENCES

1. Massoth F. E.: *Advan. Catal. Relat. Subj.* 27, 265 (1978).
2. Delmon B.: *Proc. Climax 3rd Int. Conf. Chemistry and Uses of Molybdenum* (H. F. Barry and P. C. H. Mitchell, Eds.), p. 73. Climax Molybdenum Co., London 1980.
3. Grange P.: *Catal. Rev. Sci. Eng.* 21, 135 (1980).
4. Mitchell P. C. H.: *Catalysis* (Chem. Soc. Spec. Periodic Rep., London) 4, 175 (1981).
5. Topsøe H., Candia R., Topsøe N. Y., Clausen B. S.: *Bull. Soc. Chim. Belg.* 93, 783 (1984).
6. López R., Peter R., Zdražil M.: *J. Catal.* 73, 406 (1982).
7. Peter R., Matějček V., Zdražil M.: *This Journal*, in press.
8. Givens E. N., Venuto P. B.: *A. C. S. Div. Petrol. Chem. Preprints* 15, A 183 (1970).

9. Furimsky E., Amberg C. H.: *Can. J. Chem.* **54**, 1507 (1976).
10. Daly F. P.: *J. Catal.* **51**, 221 (1978).
11. Devanneaux J., Maurin J.: *Catal.* **69**, 202 (1981).
12. Zdražil M.: *Appl. Catal.* **4**, 107 (1982).
13. Zdražil M.: *J. Catal.* **58**, 436 (1979).
14. Wei J., Prater C. D.: *Advan. Catal. Relat. Subj.* **13**, 203 (1962).
15. Smith R. L., Prater C. D.: *Chem. Eng. Prog. Symp. Ser.* **63**, 105 (1967).
16. Beránek L.: *Advan. Catal. Relat. Subj.* **24**, 1 (1975).
17. de Boer D. H., van de Borg R. J. A. M.: *Actes du Deuxième Congrès International de Catalyse, Paris 1960, Vol. 1, p. 919. Technip, Paris 1961.*
18. Hillerová E., López R., Maternová J., Peter R., Zdražil M.: *This Journal* **49**, 29 (1984).
19. Vrinat M.: *Appl. Catal.* **6**, 137 (1983).
20. Pokorný P., Zdražil M.: *This Journal* **46**, 2185 (1981).
21. Kraus J., Zdražil M.: *React. Kinet. Catal. Lett.* **6**, 475 (1977).

Translated by the author (M. Z.).